Arch. Mech., 33, 5, pp. 675–689, Warszawa 1981

Pulse load of annular plastic plates supported on both edges

D. NIEPOSTYN and A. STAŃCZYK (WARSZAWA)

A SOLUTION to the problem of dynamic bending of annular plates with various supporting conditions of both edges has been given. Motion equations have been derived and discussed on the assumption of a pulse of a uniformly distributed transversal load, determined by an arbitrary integrable function $p(t)$. A rigid-plastic model of the material, the Johanson limit state condition and the associated flow law have been assumed. Numerical analysis has been performed for loading with rectangular pressure pulse.

Podano rozwiązanie problemu dynamicznego zginania płyt pierścieniowych z różnymi warunkami podparcia obu brzegów. Równania ruchu wyprowadzono i dyskutowano przy założeniu impulsu równomiernie rozłożonego obciążenia poprzecznego, określonego dowolną całkowalną funkcją $p(t)$. Przyjęto sztywno-plastyczny model materiału, warunek stanu granicznego Johansena oraz stowarzyszone prawo płynięcia. Dla obciążenia prostokątnym impulsem ciśnienia przeprowadzono analizę numeryczną.

Приведено решение динамической задачи изгиба кольцевых плит с разными условиями опирания обоих краев. Уравнения движения выведены и обсуждены при предположении импульса равномерно распределенной поперечной нагрузки, определенной произвольной интегрируемой функцией $p(t)$. Принята жестко-пластическая модель материала, условие предельного состояния Иогансена, а также ассоциированный закон течения. Для нагружения прямоугольным импульсом давления проведен численный анализ.

1. Assumptions, formulation of the problem

THE ANALYSIS of the problem will be based upon the following assumptions:

The ideal plastic-rigid model of material. The plate under consideration assumes the plastic state according to the Johansen limit state condition

$$\Phi_{1,2} = M_r \pm M_0 = 0, \quad \Phi_{3,4} = M_\varphi \pm M_0 = 0. \tag{1.1}$$

The limit surface (1.1) is determined by the plastic potential for velocities of curvatures $\dot{k}_r$ and $\dot{k}_\varphi$

$$\dot{k}_r = -\frac{1}{a^2}\dot{w}_{,\varrho\varrho}, \quad \dot{k}_\varphi = -\frac{1}{a^2\varrho}\dot{w}_{,\varrho}. \tag{1.2}$$

The yield point does not depend upon the velocity of plastic deformations. The assumptions of the technical theory of plates remain valid.

Let a plate (Fig. 1) with the boundary conditions

$$\begin{gathered} M_r(k,t) = -\varkappa_1 M_0, \quad M_r(1,t) = -\varkappa_2 M_0 \quad (\varkappa_1, \varkappa_2 = 0 \cup 1), \\ w(k,t) = w(1,t) = 0 \end{gathered} \tag{1.3}$$

be subjected to a load determined by an arbitrary integrable function $p(t)$. We will assume uniform conditions for the beginning of the motion

$$w(\varrho, 0) = \dot{w}(\varrho, 0) = 0. \tag{1.4}$$

We will look for a complete solution. Let us assume that the plates under consideration satisfy the following conditions at any moment of the motion:

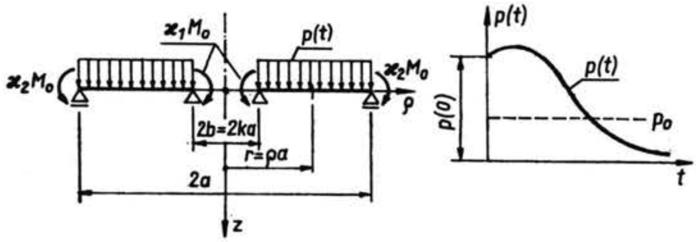

FIG. 1.

i) equations of dynamic equilibr um

$$\begin{aligned}(\varrho M_r)_{,\varrho} - M_\varphi &= \varrho a T_r,\\ \varrho a T_r &= R(k, t) b - a^2 \int_k^\varrho [p(t) - \mu \ddot{w}(\varrho, t)] \varrho d\varrho,\end{aligned} \tag{1.5}$$

where a is the outer radius of the plate, $k = b/a$ a dimensionless radius of inner edge, $\varrho = r/a$ dimensionless current radius, μ mass per unit area, $R(k, t)$ reaction of inner edge,

ii) the field of internal forces in the plate satisfies the limit state condition (1.1),

iii) the form of the motion of the plate is in conformity with the law of plastic flow and kinematic restraints,

iv) the conditions of possible discontinuities with respect to movable hinge lines $\varrho = \xi_i(t)$ are satisfied as follows

$$\begin{aligned}[\dot{w}] + \dot{\xi}_i [w_{,\varrho}] &= 0,\\ [\dot{w}_{,\varrho}] + \dot{\xi}_i [w_{,\varrho\varrho}] &= 0,\\ [\ddot{w}] + \dot{\xi}_i [\dot{w}_{,\varrho}] &= 0.\end{aligned} \tag{1.6}$$

The conditions (1.6) have been given according to [1]. Square brackets denote the discontinuities of the respective functions.

2. Problems of ultimate load carrying capacity

The problem of ultimate load carrying capacity of plates with the boundary conditions (1.2) under a uniform load on the assumption of the yield condition of maximum normal stresses has been solved in [2]. Figure 2b shows the shape of the deformation surface in the limit state corresponding to this solution. The individual plastic states in the plate

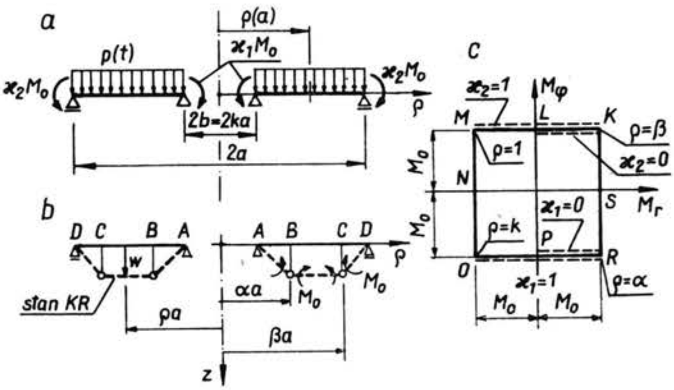

FIG. 2.

under consideration have been shown in Fig. 2c. For the KR segment we will have $\dot{k}_\varphi = 0$. From this it may be seen that during the process of plastic flow the ring BC is in translatory motion only. The limit load of the plate should be determined from the formula

$$p_0 = \frac{4M_0}{a^2}\frac{1}{\beta^2-\alpha^2}, \tag{2.1}$$

where α and β are the dimensionless coordinates of circumferential plastic bents observed in the limit state. These quantities are the solutions of the following system of non-linear algebraic equations:

$$\begin{aligned} &2(\alpha-k)^2(2\alpha+k)-3k(1+\varkappa_1)(\beta^2-\alpha^2) = 0,\\ &2(1-\beta)^2(1+2\beta)-3(1+\varkappa_2)(\beta^2-\alpha^2) = 0. \end{aligned} \tag{2.2}$$

The curves representing the $p_0a^2/4M_0$ ratio depending on the $k = b/a$ parameter for the four variants of support of edges have been shown in Fig. 3.

In the limit state of the plate under consideration, the field of internal forces is determined by the following equations:

in the region of the AB ring ($k \leqslant \varrho \leqslant \alpha$)

$$\begin{aligned} M_\varphi &= -M_0,\\ M_r &= M_0\left[1-\frac{2(\alpha-\varrho)^2(2\alpha+\varrho)}{3\varrho(\beta^2-\alpha^2)}\right],\\ T_r &= \frac{2M_0}{\varrho a}\left(1+\frac{\alpha^2-\varrho^2}{\beta^2-\alpha^2}\right); \end{aligned} \tag{2.3}$$

in the region of the BC ring ($\alpha \leqslant \varrho \leqslant \beta$)

$$\begin{aligned} M_\varphi &= M_0\left(1-2\frac{\beta^2-\varrho^2}{\beta^2-\alpha^2}\right),\\ M_r &= M_0,\\ T_r &= \frac{2M_0}{\varrho a}\left(1-\frac{\varrho^2-\alpha^2}{\beta^2-\alpha^2}\right); \end{aligned} \tag{2.3'}$$

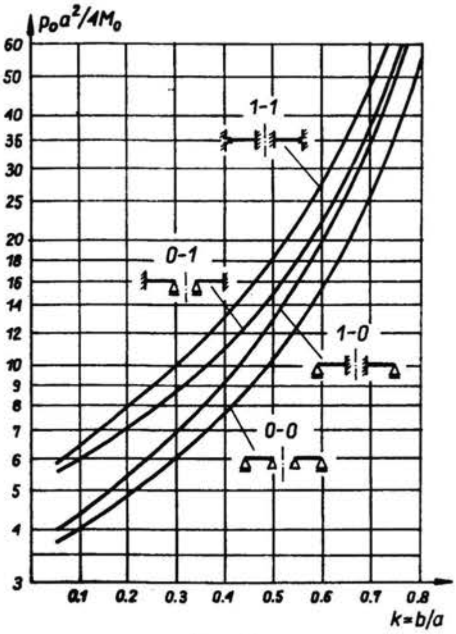

FIG. 3.

in the region of the CD ring $(\beta \leqslant \varrho \leqslant 1)$

$$M_\varphi = M_0,$$

$$M_r = M_0\left[1-\frac{2(\varrho-\beta)^2(\varrho+2\beta)}{3\varrho(\beta^2-\alpha^2)}\right], \tag{2.3''}$$

$$T_r = -\frac{2M_0}{\varrho a}\frac{\varrho^2-\beta^2}{\beta^2-\alpha^2}.$$

3. Analysis of motion of plate

The dynamic load $p(t) > p_0$ causes a motion of plate, accompanied by the formation of forces of inertia. In order to determine the proper form of the motion, numerou kinematically possible mechanisms have been analysed. In the simplest of them it has been assumed that the velocity field is similar to that encountered in the static problem of ultimate load carrying capacity (Fig. 2b). In the most complicated configuration, the motion of five annular regions with four nonsteady circumferential hinge lines has been considered. The investigation of the form of the motion for the velocity field identical to that encountered in the problem of ultimate load carrying capacity seemes to be justified since as a result of such an analysis, a range of the so-called mean values has been obtained (vide [1, 3 and 4]). From the condition of the extremum of radial moment in the internal region of the plate under consideration, the maximum medium load has been obtained.

If the loads exceed this maximum value (high load range) the motion of the plates takes place in the nonsteady velocity field.

However, the situation is quite different in the case of plates considered in this paper. It may be seen that in the problem studied, the form of the motion wherein the hinge circles are steady and occupy the positions $\varrho = \alpha$ and $\varrho = \beta$ is impossible. As it will be proved later, such positions of hinge circles lead to contradictions in acceleration fields. In consequence, the problem must be considered in a class of nonsteady problems for all loads $p(t) > p_0$. The aforementioned contradictions in the description of the motion of a plate do not occur only if the velocity field has an identical shape with that encountered in the problem of ultimate load carrying capacity provided the positions of both circumferential hinge lines are the functions of time (Fig. 4a).

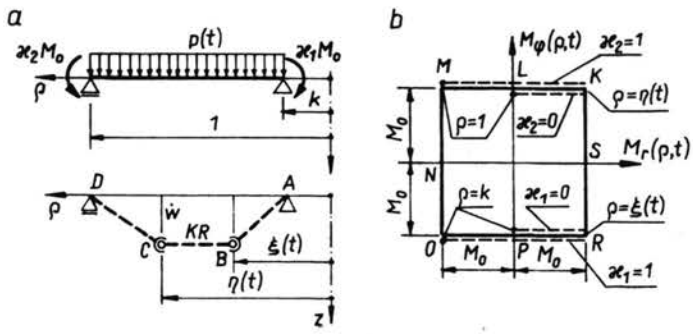

FIG. 4.

Therefore, let us assume that the action of the load $p(t)$ within the region of the plate brings about the appearance of two nonsteady circles of the positive hinges $\xi(t)$ and $\eta(t)$. Further, let us separate the three annular regions AB, BC, and CD within this plate. In consequence, we will have the following plastic states within this plate (Fig. 4b):

i) PR state ($\varkappa_1 = 0$) or OR ($\varkappa_1 = 1$)

$$M_\varphi(\varrho, t) = -M_0, \quad -\varkappa_1 M_0 \leqslant M_r(\varrho, t) \leqslant M_0, \quad k \leqslant \varrho \leqslant \xi(t); \tag{3.1}$$

ii) RK state

$$-M_0 \leqslant M_\varphi(\varrho, t) \leqslant M_0, \quad M_r(\varrho, t) = M_0, \quad \xi(t) \leqslant \varrho \leqslant \eta(t); \tag{3.1'}$$

iii) KL state ($\varkappa_2 = 0$) or KM ($\varkappa_2 = 1$)

$$M_\varphi(\varrho, t) = M_0, \quad M_0 \geqslant M_r(\varrho, t) \geqslant -\varkappa_2 M_0, \quad \eta(t) \leqslant \varrho \leqslant 1. \tag{3.1''}$$

In the region of the centre ring BC $M_r(\varrho, t) = M_0 = \text{const}$.

According to Eq. (1.5) the circumferential moment in this region must satisfy the equation

$$M_0 - M_\varphi(\varrho, t) = \xi a T_r(\xi) - \frac{p(t)a^2}{2}(\varrho^2 - \xi^2) + \frac{\mu a^2}{2}\ddot{W}(t)(\varrho^2 - \xi^2), \tag{3.2}$$

where $\ddot{W}(t)$ is a function determining the acceleration in a translatory motion ($\dot{k\varphi} = 0$) of the ring BC. Making use of the conditions on the hinge circles in Eq. (3.2)

$$M_\varphi(\xi, t) = -M_0 \quad \text{and} \quad M_\varphi(\eta, t) = M_0, \tag{3.3}$$

we will obtain the formulae for transversal forces

$$T_r(\xi, t) = -\frac{2M_0}{a\xi} \quad \text{and} \quad T_r(\eta, t) = 0 \tag{3.4}$$

and an equation for the acceleration of the region BC

$$\ddot{W}(t) = \frac{p(t)}{\mu} - \frac{4M_0}{a^2}\frac{1}{\eta^2-\xi^2}. \tag{3.5}$$

Should we make use of the relationship (2.1) in Eq. (3.5), then we may present the following:

$$\ddot{W}(t) = \frac{p(t)}{\mu} - \frac{p_0}{\mu}\frac{\beta^2-\alpha^2}{\eta^2-\xi^2}. \tag{3.6}$$

The second term on the right-hand side of Eq. (3.6) corresponds to a plastic resistance on the plate. This resistance is the greater, the nearer the hinge circles are to one another. During the motion of the plate the support zones AB and CD revolve relative to the axes passing through the supports. Linear accelerations of points lying on these lobes can be expressed by the following formulae:

$$\ddot{w}(\varrho, t) = \left[\frac{\dot{W}(t)}{\xi-k}\right]^{\cdot}(\varrho-k) \quad \text{for} \quad k \leqslant \varrho \leqslant \xi(t), \tag{3.7}$$

$$\ddot{w}(\varrho, t) = \left[\frac{\dot{W}(t)}{1-\eta}\right]^{\cdot}(1-\varrho) \quad \text{for} \quad \eta(t) < \varrho \leqslant 1. \tag{3.8}$$

Taking into account the above-mentioned expressions in the equations of equilibrium (1.5), we will obtain the following formulae for determining the distribution of radial bending moments:

i) in the zone AB

$$\varrho M_r(\varrho, t) = M_0[\varrho-k(1+\varkappa_1)] - \frac{p(t)a^2}{6}(\varrho-k)[(\varrho-k)-(\varrho+2k)-3(\xi^2-k^2)]$$
$$+\frac{\mu a^2}{12}\left(\frac{\dot{W}}{\xi-k}\right)^{\cdot}(\varrho-k)[(\varrho-k)^2(\varrho+k)-2(\xi-k)^2(2\xi+k)]; \tag{3.9}$$

ii) in the zone CD

$$\varrho M_r(\varrho, t) = -M_0(1+\varkappa_2-\varrho) - \frac{p(t)a^2}{6}(1-\varrho)[(1-\varrho)(2+\varrho)-3(1-\eta^2)]$$
$$+\frac{\mu a^2}{12}\left(\frac{\dot{W}}{1-\eta}\right)^{\cdot}(1-\varrho)[(1-\varrho)^2(1+\varrho)-2(1-\eta)^2(1+2\eta)]. \tag{3.10}$$

Integration constants have been derived from the boundary stress conditions (1.3). The reaction $R(k, t)$ has been eliminated by making use of the first equation in the set (3.4) and of the equation of transversal forces (1.5′).

Having used the conditions for the lines limiting the BC ring

$$M_r(\xi, t) = M_r(\eta, t) = M_0 \tag{3.11}$$

we will obtain two differential equations:

$$\left(\frac{\dot{W}}{\xi-k}\right)^{\cdot} = \frac{2p(t)}{\mu}\frac{2\xi+k}{(\xi-k)(3\xi+k)} - \frac{12M_0}{\mu a^2}\frac{k(1+\varkappa_1)}{(\xi-k)^3(3\xi+k)}, \tag{3.12}$$

$$\left(\frac{\dot{W}}{1-\eta}\right)^{\cdot} = \frac{2p(t)}{\mu}\frac{1+2\eta}{(1-\eta)(1+3\eta)} - \frac{12M_0}{\mu a^2}\frac{1+\varkappa_2}{(1-\eta)^3(1+3\eta)}, \tag{3.13}$$

which, together with Eq. (3.5), constitute the system of equations for our problem.

It may now be easily proved why a steady form of deformation, wherein the hinge circles occupy a position such as that encountered in the problem of ultimate load carrying capacity is not possible. In order to prove this, we introduce $\xi(t) = \alpha$ and $\eta(t) = \beta$ in Eqs. (3.12), (3.5) and (3.13), and next use the formulae (2.1) and (2.2) in these equations. As a result, we obtain the three following expressions for accelerations:

$$\begin{aligned} \ddot{w}(\varrho, t) &= \frac{p(t)-p_0}{\mu}\left(1+\frac{\alpha+k}{3\alpha+k}\right)\frac{\varrho-k}{\alpha-k}, && k \leqslant \varrho \leqslant \alpha, \\ \ddot{W}(t) &= \frac{p(t)-p_0}{\mu}, && \alpha \leqslant \varrho \leqslant \beta, \\ \ddot{w}(\varrho, t) &= \frac{p(t)-p_0}{\mu}\left(1+\frac{1+\beta}{1+3\beta}\right)\frac{1-\varrho}{1-\beta}, && \beta \leqslant \varrho \leqslant 1. \end{aligned} \tag{3.14}$$

From these equations it follows that on the hinge circles (for $\varrho = \alpha$ and $\varrho = \beta$) we will obtain discontinuous accelerations, being in contradiction with the condition (1.6″) from which it follows that accelerations on the steady hinge lines should be continuous. This condition is satisfied then and only then when the loads $p(t) = p_0$. In such a case $\ddot{W}(t) = 0$; we shall hence pass to the ultimate load carrying capacity.

4. General solution

The motion on a plate under an arbitrary pulse load is fully described by the three functions $W(t)$, $\xi(t)$ and $\eta(t)$. We will rewrite the system of equations for the determination of these functions in a form more convenient for diffrentation. To this aim it is only necessary to perform the operations of differentation in Eqs. (3.12) and (3.13) and then to substitute in them, in turn, the expressions (3.5). Consequently we will obtain

$$\frac{\mu a^2}{4M_0}\frac{\dot{W}}{\xi-k}\dot{\xi} = -\frac{p(t)a^2}{4M_0}\frac{\xi+k}{3\xi+k} + \left[\frac{3k(1+\varkappa_1)}{(3\xi+k)(\xi-k)^2} - \frac{1}{\eta^2-\xi^2}\right], \tag{4.1}$$

$$\frac{\mu a^2}{4M_0}\frac{\dot{W}}{1-\eta}\dot{\eta} = \frac{p(t)a^2}{4M_0}\frac{1+\eta}{1+3\eta} - \left[\frac{3(1+\varkappa_2)}{(1+3\eta)(1-\eta)^2} - \frac{1}{\eta^2-\xi^2}\right], \tag{4.1′}$$

$$\frac{\mu a^2}{4M_0}\ddot{W} = \frac{p(t)a^2}{4M_0} - \frac{1}{\eta^2-\xi^2}. \tag{4.1″}$$

The first two equations may be interpreted as equivalent to an appropriately transformed kinematic condition (1.6″). The functions on the right hand side of these equations describe the discontinuities of acceleration in the sections with instantaneous circumferential hinge lines.

Let us next consider the problem of initial conditions. By using the condition $\dot{W}(0) = 0$ in Eqs. (4.1) and (4.1') considered at the moment, $t = 0$, we will obtain a system of algebraic equations enabling the initial position of the hinge circles to be determined.

Having denoted

$$\varphi = p(0)/p_0, \quad \xi(0) = \xi_0, \quad \eta(0) = \eta_0 \tag{4.2}$$

we can rewrite this system of equations in the following form:

$$\begin{aligned} -\frac{\varphi}{\beta^2-\alpha^2}\,\frac{\xi_0+k}{3\xi_0+k}+\frac{3k(1+\varkappa_1)}{(3\xi_0+k)(\xi_0-k)^2}-\frac{1}{\eta_0^2-\xi_0^2} &= 0,\\ \frac{\varphi}{\beta^2-\alpha^2}\,\frac{1+\eta_0}{1+3\eta_0}-\frac{3(1+\varkappa_2)}{(1+3\eta_0)(1-\eta_0)^2}+\frac{1}{\eta_0^2-\xi_0^2} &= 0. \end{aligned} \tag{4.3}$$

The most effective method of solution consists in solving the equation

$$\frac{2\varphi}{\beta^2-\alpha^2}(\xi_0-k)^2\left(\frac{\xi_0}{3\xi_0+k}-\frac{\eta_0}{1+3\eta_0}\right)+3\left[\frac{k(1+\varkappa_1)}{3\xi_0+k}-\frac{(1+\varkappa_2)(\xi_0-k)^2}{(1+3\eta_0)(1-\eta_0)^2}\right] = 0, \tag{4.4}$$

where

$$\eta_0 = \left[\xi_0^2+\frac{(3\xi_0+k)(\xi_0-k)^2}{3k(1+\varkappa_1)-\dfrac{\varphi}{\beta^2-\alpha^2}(\xi_0+k)(\xi_0-k)^2}\right]^{1/2}. \tag{4.5}$$

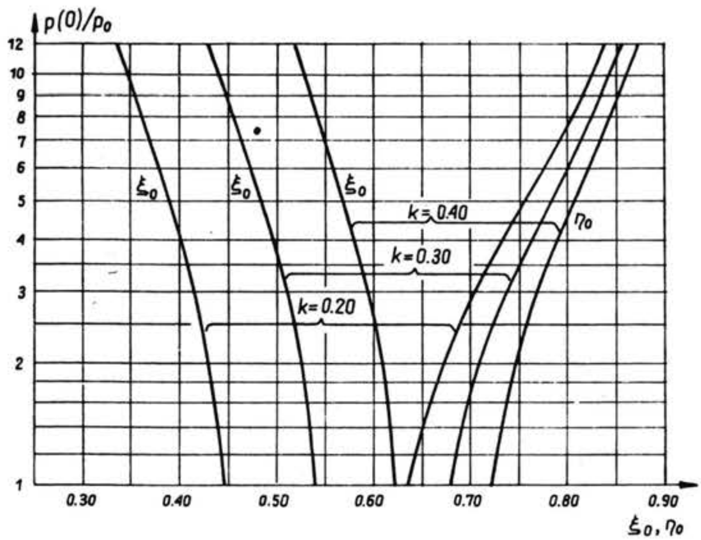

FIG. 5.

Figure 5 presents the curves of solutions of the system of equations (4.3) for a plate simply supported on both edges. The curves of the solutions for the remaining edge support variants have a similar character. There is a general regularity consisting in the fact that the greater the load $p(0)$, the closer the hinge circles are to the supports. Moreover, for $p(0) \geqslant p_0$, we always obtain $\xi_0 \leqslant \alpha$ and $\eta_0 \geqslant \beta$.

The conditions (1.4) and the roots of the system of equations (4.3) formally constitute a system of initial conditions for the system of differential equations (4.1), but they are not sufficient for numerical solution since Eqs. (4.1) and (4.1′) transformed with respect to $\dot{\xi}$ and $\dot{\eta}$ have singularity of the 0/0 type at the initial point. For this reason, in order to find the velocities $\dot{\xi}(0)$ and $\dot{\eta}(0)$, an additional analysis must be performed. To this aim we will differentiate Eqs. (4.1) and (4.1′) with respect to time and we will make use of Eq. (4.1″). After elementary transformations we will obtain the two following differential equations:

$$(4.6)\qquad \begin{aligned} &\frac{\mu a^2}{8M_0}\dot{W}\ddot{\xi}+\left[\frac{p(t)a^2}{2M_0}\frac{3\xi^2+2k\xi+k^2}{(3\xi+k)^2}+\frac{3k(1+\varkappa_1)(3\xi-k)}{(3\xi+k)^2(\xi-k)^2}+\frac{\xi(\xi-k)}{(\eta^2-\xi^2)^2}\right]\dot{\xi}\\ &\qquad\qquad -\frac{\eta(\xi-k)}{(\eta^2-\xi^2)^2}\dot{\eta}=-\frac{\dot{p}(t)a^2}{8M_0}\frac{\xi^2-k^2}{3\xi+k},\\ &\frac{\mu a^2}{8M_0}\dot{W}\ddot{\eta}+\left[\frac{p(t)a^2}{2M_0}\frac{3\eta^2+2\eta+1}{(1+3\eta)^2}+\frac{3(1+\varkappa_2)(3\eta-1)}{(1+3\eta)^2(1-\eta)^2}+\frac{\eta(1-\eta)}{(\eta^2-\xi^2)^2}\right]\dot{\eta}\\ &\qquad\qquad -\frac{\xi(1-\eta)}{(\eta^2-\xi^2)^2}\dot{\xi}=\frac{\dot{p}(t)a^2}{8M_0}\frac{1-\eta^2}{1+3\eta}. \end{aligned}$$

Considering these equations at moment $t = 0$ and making use of the condition $\dot{W}(0) = 0$, we will obtain a system of algebraic equations with respect to $\dot{\xi}(0)$ and $\dot{\eta}(0)$. Solving this system and taking into account the relationships resulting from Eq. (4.6), we will find

$$(4.7)\qquad \begin{aligned} \dot{\xi}(0) &= -\frac{\dot{p}(0)a^2}{8M_0}\frac{\eta_0^2-\xi_0^2}{\Delta}\left[\frac{\xi_0+k}{3\xi_0+k}A(\xi_0,\eta_0)-\frac{\eta_0(1+\eta_0)}{1+3\eta_0}\frac{1}{\eta_0^2-\xi_0^2}\right],\\ \dot{\eta}(0) &= \frac{\dot{p}(0)a^2}{8M_0}\frac{\eta_0^2-\xi_0^2}{\Delta}\left[\frac{1+\eta_0}{1+3\eta_0}B(\xi_0,\eta_0)-\frac{\xi_0(\xi_0+k)}{3\xi_0+k}\frac{1}{\eta_0^2-\xi_0^2}\right], \end{aligned}$$

where

$$(4.7')\qquad \begin{aligned} A(\xi_0,\eta_0) &= \frac{1}{1-\eta_0}\left(\varphi\frac{\eta_0^2-\xi_0^2}{\beta^2-\alpha^2}+\frac{3\eta_0-1}{1+3\eta_0}\right)+\frac{\eta_0}{\eta_0^2-\xi_0^2},\\ B(\xi_0,\eta_0) &= \frac{1}{\xi_0-k}\left(\varphi\frac{\eta_0^2-\xi_0^2}{\beta^2-\alpha^2}+\frac{3\xi_0-k}{3\xi_0+k}\right)+\frac{\xi_0}{\eta_0^2-\xi_0^2},\\ \Delta &= A(\xi_0,\eta_0)B(\xi_0,\eta_0)-\xi_0\eta_0(\eta_0^2-\xi_0^2)^{-2}. \end{aligned}$$

The expressions (4.7′) are positive. The expressions in square brackets in Eq. (4.7) were investigated for various values of the parameters φ and k and for the remaining edge support variants. They are also positive. Hence, decisive for the signs of horizontal velocities of both hinge circles is the derivative of load at the initial moment. Now we can give the following information on the initial stage of the motion on the basis of solutions of the system of equations (4.3) and analysis of the expressions (4.7).

1. For the loads $p(0) = p_0$ plastic hinges are formed on the circles of the radii $\varrho = \alpha$ and $\varrho = \beta$. The system of equations (4.3) is then equivalent to Eqs. (2.2). The further course of the process depends on the character of the load determining function. Three cases are possible. If $p(t) < p_0$, then there is no motion in the plate. If $p(t) = p_0$, we

obtain the problem of limit load carrying capacity. If $p(t) > p_0$ and the load increases in the initial period, and then decreases, we obtain the problem of a dynamic bending under impact load. The hinge circles will then move toward the supports and the width of the middle ring BC will increase. After some time the signs $\dot{\xi}(t)$ and $\dot{\eta}(t)$ will change.

2. In case of a „blast" load $\left(p(0) > p_0 \text{ and } \int\limits_0^t p(t)dt \geqslant tp(t)\right)$, the derivative $\dot{p}(0) \leqslant 0$. The hinge circles will then move away from the supports thus decreasing the width of the ring BC. In the special case of a rectangular pulse corresponding to a blast loading, the hinge circles are immovable for the whole duration of the application of a load. Their relative motion toward each other begins at the moment when the load is being removed.

In the next phase the motion of a plate is in conformity with the system of differential equations (4.1). Radial bending moments in the support regions vary according to the expressions (3.9) and (3.10). Within the region of the centre ring BC we have, accordingly,

$$
\begin{aligned}
&M_r(\varrho, t) = M_0,\\
&M_\varphi(\varrho, t) = M_0\left(2\frac{\varrho^2-\xi^2}{\eta^2-\xi^2}-1\right) \quad (\xi(t) \leqslant \varrho \leqslant \eta(t)),\\
&T_r(\varrho, t) = \frac{2M_0}{a\varrho}\left(1-\frac{\varrho^2-\xi^2}{\eta^2-\xi^2}\right).
\end{aligned} \tag{4.8}
$$

The functions of radial moments reach the maximum values M_0 on the circles $\varrho = \xi(t)$ and $\varrho = \eta(t)$. In the region BC the circumferential moment increases from $-M_0$ for $\varrho = \xi(t)$ to M_0 for $\varrho = \eta(t)$.

The motion of plate will be terminated at the moment t_k determined by the following formula:

$$
t_k = \frac{1}{p_0}\int\limits_0^{t_k} p(t)dt. \tag{4.9}
$$

This formula is generally true for ideally rigid-plastic structures. The final positions ξ_1 and η_1 of the hinge circles corresponding to this moment can be found from the solution of the following system of equations:

$$
\begin{aligned}
&\frac{3k(1+\varkappa_1)}{(\xi_1-k)^2(3\xi_1+k)} - \frac{1}{\eta_1^2-\xi_1^2} = \frac{p(t_k)a^2}{4M_0}\frac{\xi_1+k}{3\xi_1+k},\\
&\frac{3(1+\varkappa_2)}{(1-\eta_1)^2(1+3\eta_1)} - \frac{1}{\eta_1^2-\xi_1^2} = \frac{p(t_k)a^2}{4M_0}\frac{1+\eta_1}{1+3\eta_1},
\end{aligned} \tag{4.10}
$$

which has been obtained after substituting the condition $\dot{W}(t_k) = 0$ in the equations of motion (4.1) and (4.1').

Due to the complexity of the equations describing the motion of the plate, the functions $W(t)$, $\xi(t)$ and $\eta(t)$ can be determined in a numerical way only. We will perform numerical analysis for the loads in the shape of a rectangular pulse. However, prior to presenting the results of this analysis let us make one short remark. It may be noticed that the region of the ring BC cannot be reduced to a circle, that is to such a situation where $\xi_1 = \eta_1$. Should this be the case then, firstly, we would obtain an infinite value of retardation for finite values of the load equation (4.1″) of the circle $B = C$ and, secondly, the transversal force on the above mentioned circle would be discontinuous. Therefore, at the moment of the termination of motion some plane plasticized region would remain in the plate in the radial direction with non-full circumferential plasticizing. Maximum permanent deflection in that region can be calculated according to the same rule independently of the type of the load

$$w(t_k) = \int_0^{t_k} \left[\int p(t)dt\right]dt - \frac{4M_0}{\mu a^2}\int_0^{t_k}\left[\int \frac{dt}{\eta^2-\xi^2}\right]dt. \tag{4.11}$$

5. Rectangular pressure pulse

In the case of a rectangular pressure pulse the load is determined by a discontinuous function. In the connection, two phases must be distinguished in the motion of the plate. In the first phase at the time interval $0 \leqslant t \leqslant T$ plate is under the steady load p. In the second phase, the load is equal to zero.

5.1. Phase I, $0 \leqslant t \leqslant T$

In accordance with Eq. (4.7), the horizontal velocities $\dot{\xi}(0) = \dot{\eta}(0) = 0$. The hinge circles are steady and occupy the position ξ_0 and η_0, derived from the solution of the system of equations (4.3). The graphical form of solutions for the simply-supported plate for $k = 0.20$; 0.30 and 0.40 in terms of $\varphi = p(0)/p_0$ is shown in Fig. 5. The first two equations of the system (4.1) are satisfied as identities. The ring BC moves downward in a uniformly accelerated motion with uniform initial conditions.

By integrating twice the second equation in the set (4.1) and using the formulae (3.7) and (3.8), we will find the deflection

$$\frac{\mu a^2}{4M_0} w(\varrho, t) = \begin{cases} \frac{1}{2}\ddot{W}_0 \frac{\varrho-k}{\xi_0-k} t^2, & k \leqslant \varrho \leqslant \xi_0, \\ \frac{1}{2}\ddot{W}_0 t^2, & \xi_0 \leqslant \varrho \leqslant \eta_0, \\ \frac{1}{2}\ddot{W}_0 \frac{1-\varrho}{1-\eta_0} t^2, & \eta_0 \leqslant \varrho \leqslant 1, \end{cases} \tag{5.1}$$

where

$$\ddot{W}_0 = \frac{\varphi}{\beta^2-\alpha^2} - \frac{1}{\eta_0^2-\xi_0^2} \tag{5.2}$$

is dimensionless acceleration of the region BC.

On the steady hinge circles there will appear discontinuities of the inclination angle of the normal to the section and discontinuities of velocity of circumferential curvature. The above mentioned discontinuities reach maximum value at the end of the first phase and remain unchanged during the further motion of the plate. Within the first phase the field of internal forces in the plate (3.9), (3.10) and (4.8) is independent of time.

5.2. Phase II, $T < t < t_k$

Upon removal of the load the hinge circles are no longer steady. Assuming $p = 0$ in the equations of motion, we will obtain

$$
\begin{aligned}
\dot{\xi} &= \left[\frac{3k(1+\varkappa_1)}{(3\xi+k)(\xi-k)} - \frac{\xi-k}{\eta^2-\xi^2}\right] \Big/ \frac{\mu a^2}{4M_0}\dot{W},\\
\dot{\eta} &= -\left[\frac{3(1+\varkappa_2)}{(1+3\eta)(1-\eta)} - \frac{1-\eta}{\eta^2-\xi^2}\right] \Big/ \frac{\mu a^2}{4M_0}\dot{W},\\
\frac{\mu a^2}{4M_0}\ddot{W} &= -\frac{1}{\eta^2-\xi^2}.
\end{aligned}
\tag{5.3}
$$

The initial conditions for the system of differential equations (5.3) result from the end of the first phase. Therefore

$$
\frac{\mu a^2}{4M_0}\dot{W}(T) = \ddot{W}_0 T, \quad \frac{\mu a^2}{4M_0}W(T) = \frac{1}{2}\ddot{W}_0 T^2, \quad \xi(T) = \xi_0, \quad \eta(T) = \eta_0.
\tag{5.4}
$$

Having substituted Eq. (5.4) in Eqs. $(5.3)_{1,2}$ we will obtain explicit information about the direction of the motion of the hinge line at the beginning of the second phase of motion:

$$
\begin{aligned}
\dot{\xi}(T_+) &= \frac{\varphi}{\beta^2-\alpha^2}\,\frac{\xi_0+k}{3\xi_0+k}\,\frac{1}{\ddot{W}_0 T} > 0,\\
\dot{\eta}(T_+) &= -\frac{\varphi}{\beta^2-\alpha^2}\,\frac{1+\eta_0}{1+3\eta_0}\,\frac{1}{\ddot{W}_0 T} < 0.
\end{aligned}
\tag{5.5}
$$

In accordance with Eq. (4.9) the motion of the plate will be terminated at the time $t_k = \varphi T$. The duration of the second phase is equal to $(\varphi-1)T$ accordingly. The final positions ξ_1 and η_1 of the hinge circles can be found from the system of equations (4.10) by substituting in them $p(t_k) = 0$. The curves of the solutions for a simply supported plate for various dimensions of the hole are presented in Fig. 6.

Irrespective of the support of edges the points corresponding to the roots of the system of equations (4.10) lie always inside a ring limited by the circles $\varrho = \alpha$ and $\varrho = \beta$. For this reason the hinge circles do not coincide with bents encountered in the problem of ultimate load carrying capacity. In consequence, in plates supported on both edges there is no phase of a rigid rotation characteristic of the solutions of dynamic bending of plates supported on one edge only.

The equations of motion (5.3) have been integrated numerically for all the four edge support variants [5] and the hole radii varying within the range $k \in [0.2, 0.5]$. Loads varied within the range $p \in [2p_0;\ 15p_0]$. The Runge–Kutta–Gill method of the fourth order has been used. The integration step has been assumed equal to 1/250 of the duration of the second phase. The results of the numerical analysis will be discussed on the basis of an example of a simply supported plate assuming that $p = 10p_0$ and $k = 0.20$. The presented example is also representative for the remaining edge support variants.

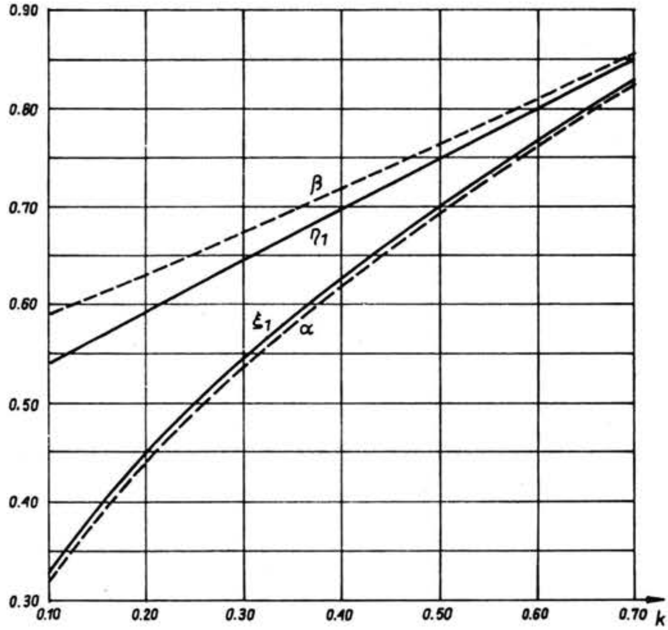
0.90
0.80
0.70
0.60
0.50
0.40
0.30
0.10
0.20
0.30
0.40
0.50
0.60
0.70
k
β
η_1
ξ_1
α

FIG. 6.

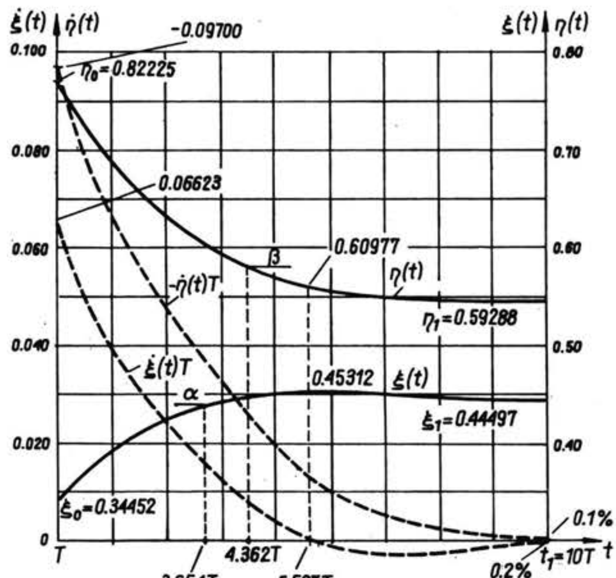
$\dot{\xi}(t)$
$\dot{\eta}(t)$
$\xi(t)$
$\eta(t)$
-0.09700
$\eta_0 = 0.82225$
0.06623
0.60977
β
$-\dot{\eta}(t)T$
$\eta(t)$
$\eta_1 = 0.59288$
$\dot{\xi}(t)T$
0.45312
$\xi(t)$
α
$\xi_1 = 0.44497$
$\xi_0 = 0.34452$
0.1%
0.2%
$t_1 = 10T$
t
T
3.654T
4.362T
5.587T
0.100
0.080
0.060
0.040
0.020
0
0.80
0.70
0.60
0.50
0.40

FIG. 7.

Horizontal motion of hinge circles has been presented in Fig. 7. Horizontal velocities have been shown with dashed lines and their integers, with full lines. The velocity of the circle $C(\varrho = \eta(t))$ is always negative. The motion of the circle B is more complicated. For about half the phase it moves away from the inner edge and then reverses. However, because of the decreasing width of the ring BC for the whole duration of the second phase the retardation of the motion of this ring is even greater. In the final phase of the motion the velocities $\dot{\xi}$ and $\dot{\eta}$ are equal to zero (with very good accuracy, errors being as low as 0.2% and 0.1% of the initial values).

Also transversal velocity at the end of the motion has been determined with high accuracy, the error being as low as 2% of the initial value; this is a consequence of a singularity of the 0/0 type, included in Eqs. (5.3) at the moment t_k. In spite of the above mentioned singularity, in case of the method of integration of the equations of motion being used, the error in the estimate of the value $\dot{W}(t)_k$ is always insignificant independently of the supporting conditions.

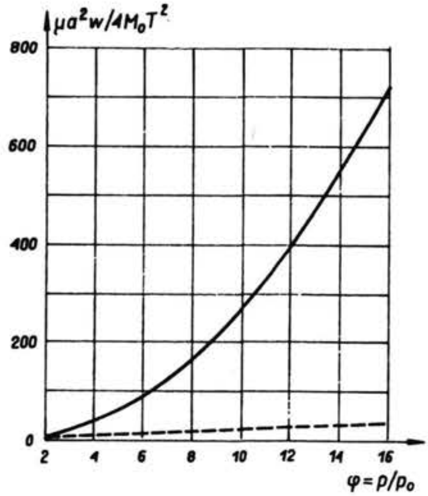

FIG. 8.

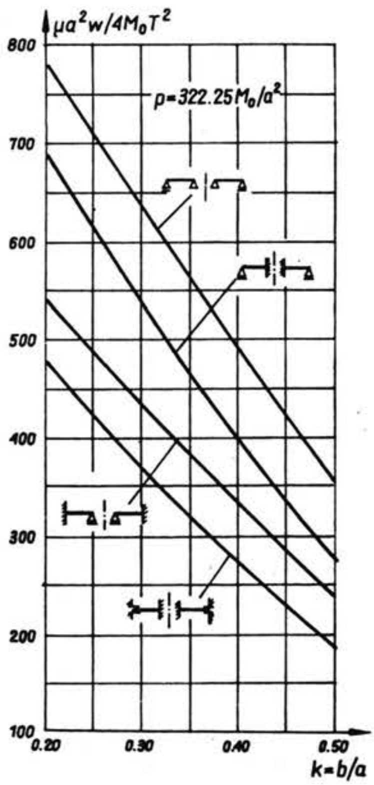

FIG. 9.

Figure 8 shows the curve of maximum permanent deflections $k = 0.20$ depending the load. The deflections at the end of the first phase are shown with dashed lines. The influence of this phase upon the final deflections decreases with an increasing load. Within the load range $p \in [2p_0;\ 5p_0]$ the deflection w_I decreases from 48% to 18% w_{max}. A more detailed analysis of deflections indicated that the percentage of w_I in final deflection is almost independent of the size of the plate hole and is mainly due to the load. Hence, in case of a dynamic load only three times as great as the limit one, there is a clearly visible decisive (quantitative) influence of the phase of nonsteady hinge lines.

The comparison of final deflections depending on boundary conditions and hole size has been visualized in Fig. 9. The curves of deflections lie in reversed order to the lines determining the ratio $p_0 a^2/4M_0$ (Fig. 2). The deflections of fixed plates are 1.6 to 1.8 times smaller than those of freely supported plates. In the case of plates with mixed boundary conditions, the deflections of plates with fixed outer edge are smaller.

6. Conclusions

Deformation of rigid-plastic plates which are supported on both edges under pulse loads is substantially different from the deformation of plates supported on one edge only. In the case of the former, there is neither a range of medium loads nor a final phase of rigid rotation characteristic of the plates supported on one edge only. In the case of plates supported on both edges, the rotation terminates in the phase of movable hinge lines. This very phase is decisive for the amount of permanent deflection.

Extremely high accuracy of numerical calculations and very small errors observed confirm that a proper method of integration of the equations of motion has been used. This method has also been tested on the basis of an example of a triangular pressure pulse. Here also this test yielded positive results. An insignificant influence of the form of pressure variations upon the value of the final deflection of the plates has been proved. Should identical values of pulse acting on the plate be assumed, then final deflection due to a triangular pulse would be greater by almost 5% than that due to a rectangular pulse.

References

1. H. G. HOPKINS, W. PRAGER, *On the dynamics of plastic circular plates*, ZAMP, **5**, 4, 317–330. 1954.
2. D. NIEPOSTYN, *Nośność graniczna płyt kołowo-symetrycznych* (Ultimate load carrying capacity of circular-symmetric plates), Bibl. Inż. i Bud., Arkady 1963.
3. P. PERZYNA, *Dynamic load carrying capacity of a circular plate*, Arch. Mech., **10**, 5, 635–647, 1958.
4. Z. MRÓZ, *Plastic deformations of annular plates under dynamic loads*, Arch. Mech., **10**, 4, 499–516, 1958.
5. A. E. STAŃCZYK, *Pierścieniowe płyty plastyczne obciążone impulsem ciśnienia* (Annular plastic plates under pressure pulse), Doctoral Thesis, WAT 1977.

Received September 22, 1980.